miR-146a-5p protects against renal injury in MRL/lpr mice via improvement of the Treg/Th17 imbalance by targeting the TRAF6/NF-κB axis

JIAJIA TENG[1*], FENG YANG[2*] and XIAOLING LI[2]

Departments of [1]Nephropathy and [2]Rheumatology, Yantai Hospital of Traditional Chinese Medicine, Yantai, Shandong 264001, P.R. China

Received June 25, 2022; Accepted November 2, 2022

DOI: 10.3892/etm.2022.11720

Abstract. Dysregulated microRNA (miRNA or miR) expression is an important cause of immune homeostasis disorder in patients with systemic lupus erythematosus and lupus nephritis (LN). The present study evaluated the possibility of using miR-146a-5p as a therapeutic target for treating LN. The effects of miR-146a-5p on lupus syndrome in MRL/lpr mice were evaluated. MRL/lpr mice were injected with miR-146a-5p agomir (M146AG) or agomir negative control (NC). Renal function index, pathology and protein expression levels of inflammatory factors in MRL/lpr mice were evaluated after M146AG or agomir NC treatment. Reverse transcription-quantitative PCR, western blotting and immunofluorescence were used to assess the effect of M146AG on mRNA and protein expression levels of (tumor necrosis factor receptor-associated factor 6) TRAF6/NF-κB axis components. A luciferase dual reporter system was used to assess the mechanism of regulation of TRAF6/NF-κB axis expression. Finally, flow cytometry was used to assess the regulatory effect of M146AG on regulatory T cell (Treg)/T helper 17 (Th17) balance. The findings demonstrated that M146AG ameliorated renal lesions and the inflammatory response in MRL/lpr mice. TRAF6 was demonstrated to be targeted and significantly negatively regulated by miR-146a-5p. M146AG intervention significantly increased expression of miR-146a-5p and significantly downregulated the mRNA and protein expression levels of TRAF6 and NF-κB in $CD4^+$ T cells of MRL/lpr mice. Furthermore, M146AG intervention alleviated Treg/Th17 imbalance in MRL/lpr mice peripheral blood. The present findings demonstrated that M146AG improved Treg/Th17 imbalance and alleviated renal lesions in MRL/lpr mice by targeting the TRAF6/NF-κB axis. This may provide a new theoretical basis for the clinical diagnosis and treatment of LN.

Correspondence to: Dr Xiaoling Li, Department of Rheumatology, Yantai Hospital of Traditional Chinese Medicine, 39 Xingfu Road, Zhifu, Yantai, Shandong 264001, P.R. China
E-mail: xiaoling2022l@163.com

*Contributed equally

Abbreviations: SLE, systemic lupus erythematosus; miRNA, microRNA; TNF-α, tumor necrosis factor-α; BUN, blood urea nitrogen; LN, lupus nephritis; SCr, serum creatinine; M146AG, miR-146a-5p agomir; IFN-γ, interferon-γ; TRAF6, tumor necrosis factor receptor-associated factor 6; NF-κB, nuclear factor κB; Treg, regulatory T cell; Th17, T helper 17; H&E, hematoxylin and eosin

Key words: miR-146a-5p, TRAF6, NF-κB, lupus nephritis, Treg/Th17

Introduction

Systemic lupus erythematosus SLE is a complicated inflammatory autoimmune disease. SLE frequently affects multiple systems in the body, with the kidney being one of the most commonly involved organs (1). Lupus nephritis (LN) affects 40-70% of patients with SLE and has become a major risk factor for end-stage renal disease and death (2). Previous studies have reported that release of free radicals and inflammatory cytokines, as well as an imbalance in T cell metabolism and subsets, are the primary causes of autoimmune disease in patients with SLE (3,4).

Inflammatory signalling disorders, hyperactivation of effector cell subtypes and autoantibody production have been reported as causes of SLE (5-7). Previous studies have reported that as an important element of the effector and regulatory immune responses, T cell dysfunction is widespread in patients with SLE (8,9). Emerging evidence suggests that the imbalance of T helper 17 (Th17) and regulatory T cells (Tregs) serves an important role in the pathogenesis of SLE (8,10). Increased numbers of Th17 cells have been reported to serve a key role in the pathogenesis of SLE and LN (11,12). Moreover, blocking IL-17 is reported to be a promising treatment strategy for SLE (13). However, based on the reduction and dysfunction of Treg in patients with SLE, using Treg as a therapeutic target is also expected to alleviate SLE (14). Therefore, it may be an effective strategy to treat SLE and LN by correcting Treg/Th17 imbalance.

MicroRNAs (miRNAs or miRs), a class of single-stranded small non-coding RNAs with lengths ranging from 19 to 23 nucleotides, typically regulate the expression of their

target gene by binding to the 3'-untranslated region (3'-UTR) of mRNAs (15,16). Previous studies have reported that miRNAs are important in the regulation of immune homeostasis and abnormal miRNA expression has been reported in patients with autoimmune disease (17,18). A recent study reported that compared with healthy volunteers, miRNA in patients with SLE was differentially expressed and may be a promising biological target for SLE treatment (19). miR-199a-5p alleviates SLE by promoting splenic $CD4^+$ T cell senescence (20). miR-654 treatment decreases macrophage migration inhibitory factor expression and downstream inflammatory cytokine production, which is reported to improve murine LN (21). Numerous studies have reported that miR-146a underexpression contributes to changes in the type I interferon (IFN) pathway in patients with SLE (22,23). Furthermore, administration of miR-146a relieves renal injury in mice with SLE (24); however, the underlying mechanism is not clear. Previous studies have reported that miRNA regulates the proportion of Treg/Th17 subsets *in vivo* and *in vitro* and serves an immunotherapeutic role in autoimmune diseases (25,26). To the best of our knowledge, however, the immunotherapeutic action of SLE by correction of the Treg/Th17 imbalance via miRNA supplementation, has been rarely reported (27).

In the present study, the regulatory effect of miR-146a-5p on differentiation of Treg/Th17 in MRL/lpr mice was assessed to evaluate whether miR-146a-5p may be a potential therapeutic target for treatment of SLE-induced renal lesions.

Materials and methods

Animals and groups. A total of 30 female MRL/lpr mice (weighing 37.9±1.5 g age, 8 weeks) were purchased from Shanghai SLAC Laboratory Animal Co., Ltd. and housed in a specific-pathogen-free laboratory under standard humidity (40-60%) and temperature (25˚C), with a 12/12-h light/dark cycle and with free access to standard diet and water. The Ethics Board of Yantai Hospital of Traditional Chinese Medicine approved all experimental procedures (approval no. 2021-09). The mice received humane care and all efforts were made to alleviate suffering.

MRL/lpr mice were randomly divided into three groups (n=10/group) as follows: i) Vehicle (VEH); ii) miR-146a-5p agomir (M146AG) and iii) agomir negative control (NC) (Fig. 1A). At the age of 10-13 weeks, the MRL/lpr mice in the M146AG group and NC group were administered 20 nmol M146AG or M146AG NC in 0.2 ml saline weekly via injection into the tail vein. MRL/lpr mice in the VEH group were injected with equal volumes of saline via the tail vein on a weekly basis. All mice were sacrificed 1 week after the last injection. Guangzhou RiboBio Co., Ltd. synthesized the M146AG and M146AG NC; sequences used are presented in Table SI.

Urine samples (500 μl) were collected once /week and centrifuged at 3,000 x g for 15 min at 4˚C; supernatant was stored at -80˚C until use for urinary protein assessment. At the end of the experiment mice were anesthetized using ether and sacrificed using exsanguination via the aorta, with blood samples (500 μl) taken from the abdominal aorta. To collect serum, the blood was centrifuged at 3,000 x g for 15 min at 4˚C. Mice were confirmed dead when there was no autonomous respiration, no reflex activity and no heart activity. The kidneys were dissected, with the left kidney used for pathological analysis and the right kidney used for western blotting. Separated serum and kidney were stored at -80˚C until use in subsequent experiments.

Assessment of kidney function. Blood urea nitrogen (BUN) and serum creatinine (SCr) concentrations were assessed using commercially available Urea Nitrogen (BUN) Test (cat. no. C013-2-1; Nanjing Jiancheng Bioengineering Institute) and Creatinine (Cr) Assay kit (cat. no. C011-2-1; Nanjing Jiancheng Bioengineering Institute), respectively. The manufacturer's instructions for the corresponding assay kit were precisely followed.

Histological examination. Renal tissue was fixed using 10% formaldehyde for 24 h at 4˚C, embedded in paraffin, cut into 4 μm sections and mounted on slides. The prepared slides were deparaffinized twice in xylene at room temperature and rehydrated using an ethanol gradient before being stained independently with Masson's trichrome (5 min, room temperature) and hematoxylin and eosin (H&E) (5 min, room temperature). Tissue injury was evaluated blindly and rated using a glomerular damage score, as previously described (28). The severity of glomerulonephritis was graded on a 0-4 scale as follows: 0, normal; 1, mild increase in mesangial cellularity and matrix; 2, moderate increase in mesangial cellularity and matrix, with thickening of the glomerular basement membrane (GBM); 3, focal endocapillary hyper cellularity with obliteration of capillary lumina and a substantial increase in the thickness and irregularity of the GBM and 4, diffuse endocapillary hyper cellularity, segmental necrosis, crescents and hyalinized end-stage glomeruli.

Masson's trichrome staining was used to evaluate the area of renal interstitial fibrosis according to the manufacturer's protocol (cat. no. G1340, Beijing Solarbio Science & Technology Co., Ltd.) (29). A DM4000 light microscope was used to obtain images (Leica Microsystems GmbH). ImageJ (version 1.53; National Institutes of Health) was used to calculate fibrosis as the percentage of blue collagen-stained area relative to total tissue in each field of view as follows: Renal fibrosis score (%)=the area of Masson's trichrome-stained collagen (blue)/total area.

Assessment of serum cytokines. The levels of cytokines IFN-γ, IL-6, TNF-α and IL-17A were assessed in mouse serum using the Bio-Plex Pro™ Mouse Cytokine TH17 Panel A 6-Plex kit (cat. no. M6000007NY; Bio-Rad Laboratories, Inc.). The manufacturer's instructions for the corresponding assay kit were followed.

Flow cytometry. A FACSCanto II flow cytometer (BD Biosciences) and FlowJo software (version 10.7.1; Tree Star) were used to analyze the percentage of Th17 and Treg cells in peripheral blood mononuclear cells. Cells were incubated in the dark for 25 min at 4˚C with antibodies against surface markers. For intracellular staining, cells were fixed, permeabilized using Cytofix/Cytoperm kit (cat. no. 554714,

BD Biosciences) for 15 min at 4˚C and stained for 50 min at 4˚C in the dark with fluorescently labeled antibodies. The following antibodies were used: Anti-mouse CD3 APC (cat. no. MA1-81438; eBioscience; Thermo Fisher Scientific, Inc.), CD4 FITC (cat. no. MHCD0401; eBioscience; Thermo Fisher Scientific, Inc.), CD25 Percp-cy5.5 (cat. no. 45-0251-82; eBioscience; Thermo Fisher Scientific, Inc.), Foxp3 PE (cat. no. 12-5773-82; eBioscience; Thermo Fisher Scientific, Inc.) and IL-17 PE (cat. no. 12-7178-42; eBioscience; Thermo Fisher Scientific, Inc.).

Immunofluorescence. Immunofluorescence was performed as previously described (30). Briefly, $CD4^+$ T cells were fixed using 4% paraformaldehyde at room temperature for 30 min, washed with PBS and blocked using 0.3% Triton X-100, 10% normal goat serum (cat. no. SL038, Beijing Solarbio Science & Technology Co., Ltd) and 1% bovine serum albumin (cat. no. S9020, Beijing Solarbio Science & Technology Co., Ltd) at room temperature for 2 h. Cells were treated at 4˚C overnight with primary antibodies against tumor necrosis factor receptor-associated factor 6 (TRAF6; 1:400; cat. no. 8028, Cell Signaling Technology, Inc.) and nuclear factor (NF)-κB (1:400; cat. no. 6956, Cell Signaling Technology, Inc.). After adding fluorescently labeled goat anti-mouse IgG (DyLight 549; 1:200; cat. no. ab96881; Abcam) and goat anti-rabbit IgG (DyLight 488; 1:200; cat. no. ab96899; Abcam) secondary antibodies, samples were incubated at room temperature for 2 h. DAPI (cat. no. 4083, Cell Signaling Technology, Inc) was used as a nuclear counterstain and samples were incubated at room temperature for 2 min. The images were obtained using a LSM880 fluorescent microscope with Airyscan (Zeiss GmbH) and analyzed using ImageJ (version 1.53; National Institutes of Health).

Western blotting. Western blot analysis was performed as described previously (31,32). Briefly, $CD4^+$ T cells were lysed for 30 min on ice using RIPA buffer (cat. no. R0010; Beijing Solarbio Science & Technology Co., Ltd.) containing 1% phenylmethanesulfonyl fluoride (cat. no. P0100; Beijing Solarbio Science & Technology Co., Ltd.). The protein content was quantified using a BCA protein assay kit (cat. no. PC0020; Beijing Solarbio Science & Technology Co., Ltd). SDS-PAGE was performed on 5-15% linear acrylamide gradient gel (10 μg protein/lane). After transferring proteins onto PVDF membranes, the membranes were blocked for 2 h at room temperature using 5% skimmed milk powder. The membranes were then incubated overnight at 4˚C with primary antibodies as follows: TRAF6 (1:3,000; cat. no. 8028; Cell Signaling Technology, Inc.), NF-κB (1:3,000; cat. no. 8242; Cell Signaling Technology, Inc.), β-actin (1:5,000; cat. no. 4970; Cell Signaling Technology, Inc.), FoxP3 (1:3,000; cat. no. 12632; Cell Signaling Technology, Inc.) and IL-17A (1:3,000; cat. no. 13838; Cell Signaling Technology, Inc.). The membranes were incubated with an anti-rabbit IgG (H+L) (1:5,000; cat. no. 14708, Cell Signaling Technology, Inc.) secondary antibody for 2 h at room temperature, followed by washing 3 times using TBST (20% Tween 20). The protein bands were visualized using developer a ECL kit (cat. no. P0018FS; Beyotime Institute of Biotechnology), and semi-quantitative densitometry was performed on the identified bands using Image Quant 5.2 software (Molecular Dynamics, Inc.).

RNA extraction and reverse transcription-quantitative PCR (RT-qPCR). Total RNA was isolated from the tissue samples using TRIzon Reagent (cat. no. CW0580, CoWin Biosciences) according to the manufacturer's protocol. A total of 1 μg of total RNA was reverse transcribed into cDNA at 37˚C for 60 min and 4˚C for 5 min using a First-strand cDNA Synthesis kit (cat. no. E6300L; New England BioLabs, Inc.) according to the manufacturer's protocol. qPCR assay was performed by using SYBR green dye on Step One sequence detection system (Applied Biosystems; Thermo Fisher Scientific, Inc.). The thermocycling conditions were as follows: initial predenaturation step at 95˚C for 3 min, followed by 39 cycles of 95˚C for 20 sec and 60˚C for 30 sec. The $2^{-\Delta\Delta Cq}$ method was used to assess the relative abundance (33). The internal reference used for mRNA was GAPDH and the internal reference used for miR-146a-5p was U6. Primers are presented in Table SII.

Dual-luciferase reporter gene assay. miR-146a-5p mimics/inhibitors and corresponding NC were manufactured by Guangzhou RiboBio Co., Ltd. (Table SI). The 293T cell line was used for the luciferase reporter assay. The 3'-UTR of TRAF6 which contained the predicted binding targets of miR-146a-5p (targetscan.org/vert_72/) was cloned into the c-myc luciferase reporter plasmid (Genomeditech) with either original wild-type (WT) or altered mutant sequence (MUT) at the binding sites. The 293T cells were co-transfected using 800 ng TRAF6-WT 3'-UTR or TRAF6-MUT 3'-UTR dual luciferase reporter plasmid vector and 20 μM miR-146a-5p mimic, inhibitor or NC using Lipofectamine® 2000 (Invitrogen; Thermo Fisher Scientific, Inc.). Dual-Luciferase Reporter Assay System (E1910, Promega Corporation) was used to assess *Renilla* and Firefly luciferase activity of lysed 293T cells 24 h after transfection.

Statistical analysis. Statistical analyses were performed using SPSS (version 19.0; IBM, Corp.). Three independent experiments were performed and data are presented as mean ± standard deviation. One-way analysis of variance with Tukey's post hoc test and the unpaired Student's t-test were used for comparisons between ≥3 and 2 groups, respectively. Spearman's rank correlation coefficient was used to assess the correlation between two independent samples. $P<0.05$ was considered to indicate a statistically significant difference.

Results

M146AG alleviates renal lesions in MRL/lpr mice. To evaluate the effect of M146AG on renal function parameters of MRL/lpr mice, the concentration of BUN and SCr was assessed. The levels of BUN and SCr were significantly decreased in the M146AG group compared with both the VEH and NC groups (Fig. 1B and C).

H&E and Masson staining were used to evaluate the effect of M146AG on renal histopathology of MRL/lpr mice. In the VEH and NC groups, H&E staining demonstrated glomerular swelling and extracellular matrix deposition, as well as a high level of inflammatory cell infiltration (Fig. 1D). Furthermore,

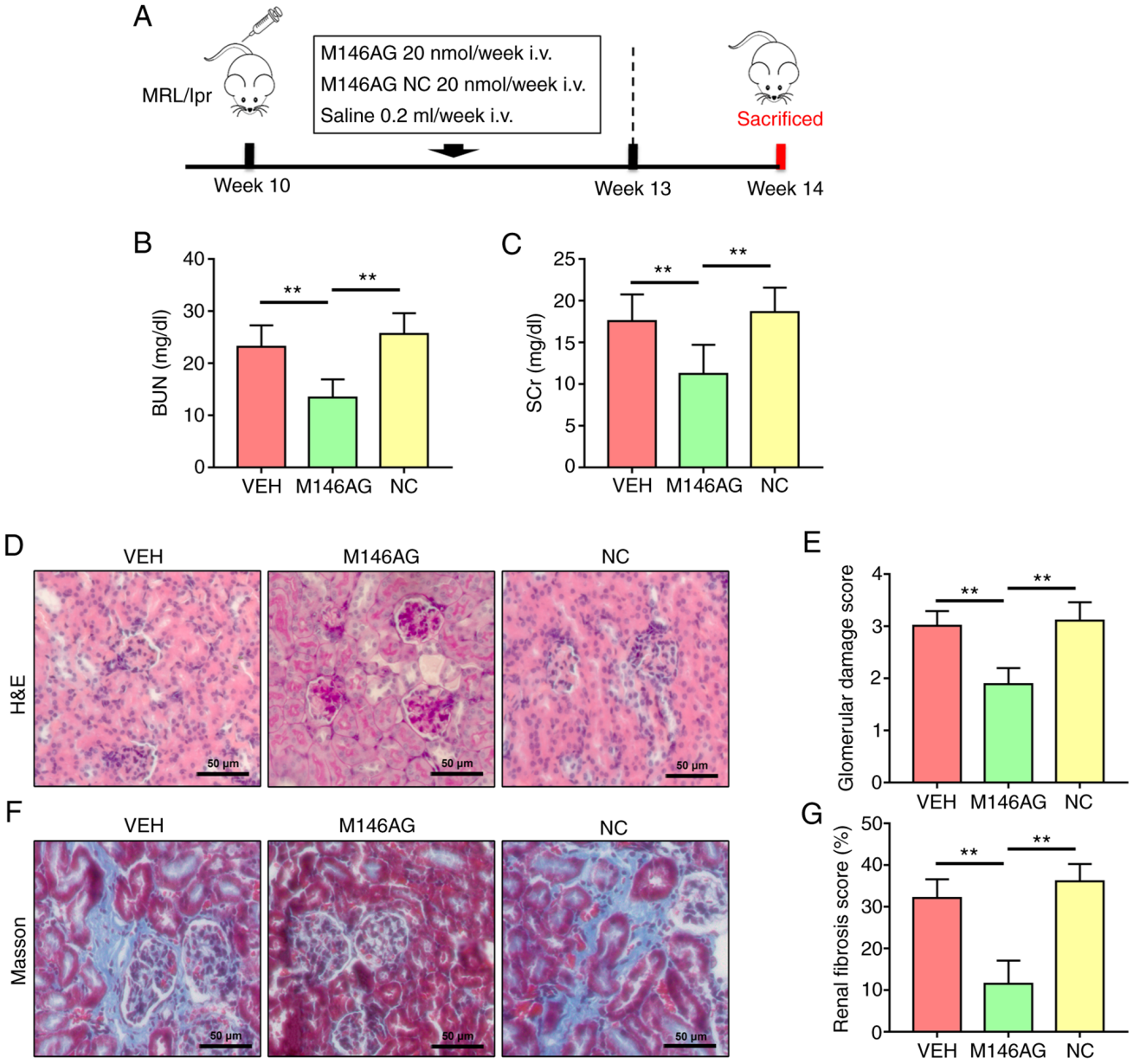

Figure 1. M146AG alleviates renal lesions in MRL/lpr mice. (A) Schematic representation of the experimental design. Renal function was assessed using (B) BUN and (C) SCr levels. (D) Representative micrographs of H&E-stained renal sections (scale bar, 50 μm). (E) Glomerular injury score. (F) Representative micrographs of Masson's trichrome-stained renal sections (scale bar, 50 μm). (G) Renal fibrosis score. All data are presented as the mean ± standard deviation. **P<0.01. i.v., intravenous; VEH, vehicle; NC, negative control; miR, microRNA; M146AG, miR-146a-5p agomir; H&E, hematoxylin and eosin; BUN, blood urea nitrogen; SCr, serum creatinine.

Masson staining demonstrated that levels of renal interstitial fibrosis in the VEH and NC group were markedly higher than those in the M146AG group (Fig. 1F). However, M146AG treatment significantly alleviated the glomerular damage and renal interstitial fibrosis scores in MRL/lpr mice compared with both the VEH and NC groups (Fig. 1D-G). These results indicated that M146AG improved renal lesions in MRL/lpr mice.

M146AG inhibits expression of inflammatory factors in the serum and renal tissue of MRL/lpr mice. The effect of M146AG on protein and mRNA expression levels of inflammatory factors in serum and renal tissue of MRL/lpr mice was assessed. Protein expression levels of serum inflammatory factors IL-6, IL-17A, TNF-α and IFN-γ were significantly decreased following M146AG intervention compared with the VEH and NC groups (Fig. 2A-D). Similarly, mRNA expression levels of inflammatory markers IL-6, IL-17A, TNF-α and IFN-γ were also significantly decreased in the renal tissues of the M146AG group compared with the VEH and NC groups (Fig. 2E-H). These results demonstrated that M146AG alleviated the inflammatory response in MRL/lpr mice.

M146AG regulates mRNA expression levels of miR-146a-5p and the TRAF6/NF-κB axis components in CD4$^+$ T cells of MRL/lpr mice. To evaluate the potential molecular mechanisms by which M146AG alleviated renal lesions in MRL/lpr mice, expression levels of miR-146a-5p and mRNA

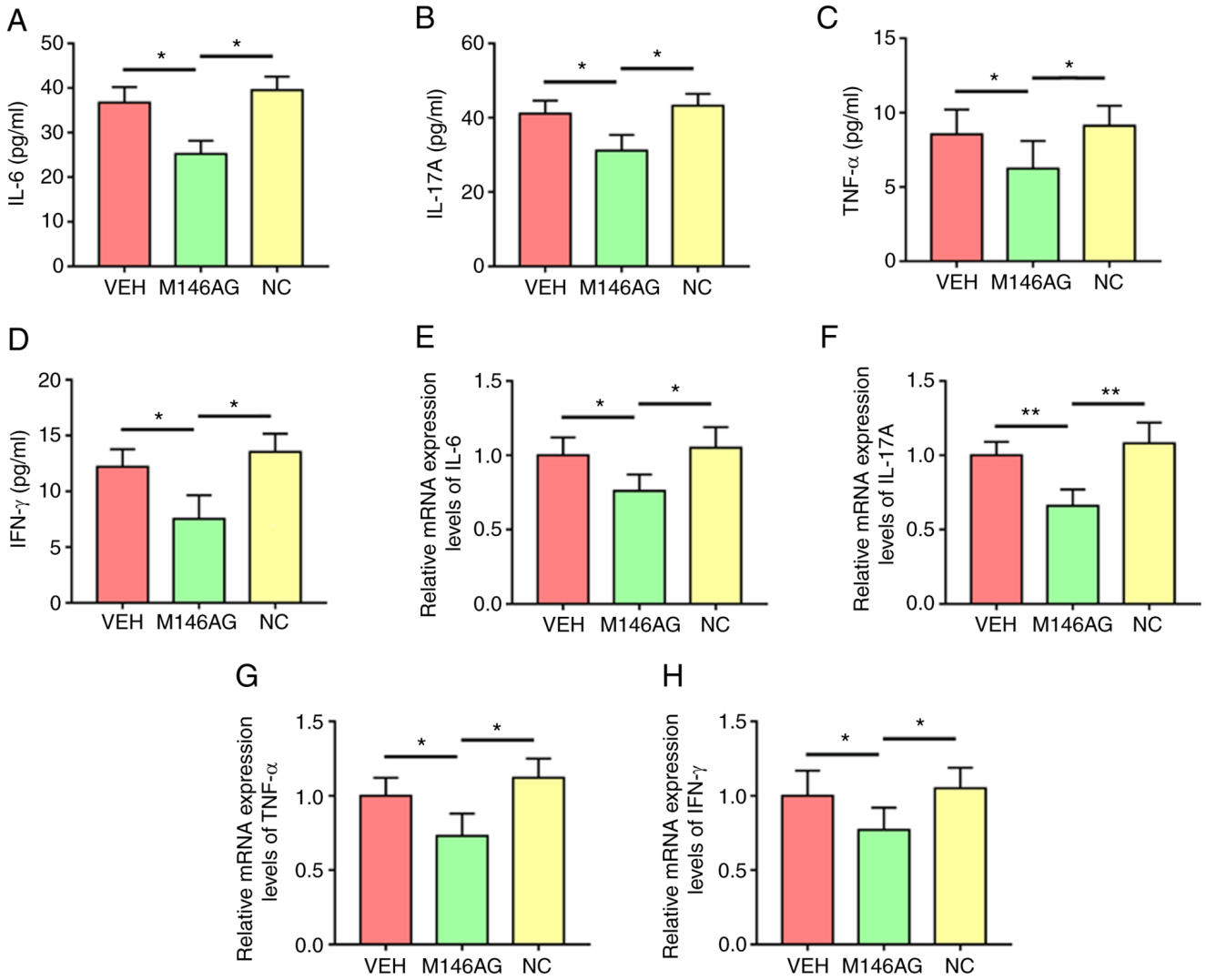

Figure 2. M146AG inhibits mRNA and protein expression levels of inflammatory factors in serum and renal tissue of MRL/lpr mice. Protein concentrations of (A) IL-6, (B) IL-17A, (C) TNF-α and (D) IFN-γ in serum of MRL/lpr mice. Relative mRNA expression levels of (E) IL-6, (F) IL-17A, (G) TNF-α and (H) IFN-γ in the renal tissue of MRL/lpr mice. All data are presented as the mean ± standard deviation. *P<0.05 and **P<0.01. VEH, vehicle; NC, negative control; miR, microRNA; M146AG, miR-146a-5p agomir.

and protein expression levels of the TRAF6/NF-κB axis components in CD4^{+} T cells were assessed. The expression of miR-146a-5p was significantly increased in CD4^{+} T cells in the M146AG treatment group compared with the VEH and NC groups (Fig. 3A). Furthermore, compared with the VEH and NC groups, mRNA and protein expression levels of TRAF6 and NF-κB were significantly decreased in CD4^{+} T cells with M146AG treatment (Fig. 3B-F). Subsequent microscopic analysis of TRAF6 and NF-κB expression levels further demonstrated the downregulate in protein expression levels in CD4^{+} T cells of MRL/lpr mice after M146AG treatment (Fig. 3G). These data indicated that M146AG intervention inhibited mRNA and protein expression levels of the TRAF6/NF-κB axis components by upregulating expression of miR-146a-5p in the CD4^{+} T cells of MRL/lpr mice.

miR-146a-5p directly targets TRAF6. Potential binding sites between miR-146a-5p and TRAF6-3'-UTR sequences were assessed using Targetscan (Fig. 4A). To evaluate if miR-146a-5p influenced TRAF6 expression levels by targeting its 3'-UTR, a luciferase reporter system was constructed. Compared with the NC group, miR-146a-5p mimic significantly decreased luciferase activity, whereas miR-146a-5p inhibitor treatment significantly increased relative luciferase activity compared with the NC group (Fig. 4B). Furthermore, when the seed sequence of the miR-146a-5p binding sites was altered, the effect of miR-146a-5p on luciferase activity was not demonstrated (Fig. 4B). Expression levels of miR-146a-5p in 293T cells were significantly increased compared with the NC. RT-qPCR demonstrated significantly lower TRAF6 mRNA expression levels in cells treated with miR-146a-5p mimics compared with NC; however, significantly increased TRAF6 mRNA expression levels were demonstrated in cells treated with miR-146a-5p inhibitor compared with NC (Fig. 4C). These results demonstrated that miR-146a-5p targeted and negatively regulated TRAF6 expression.

M146AG improves the Treg/Th17 imbalance in MRL/lpr mice. To elucidate the mechanism of M146AG-mediated regulation

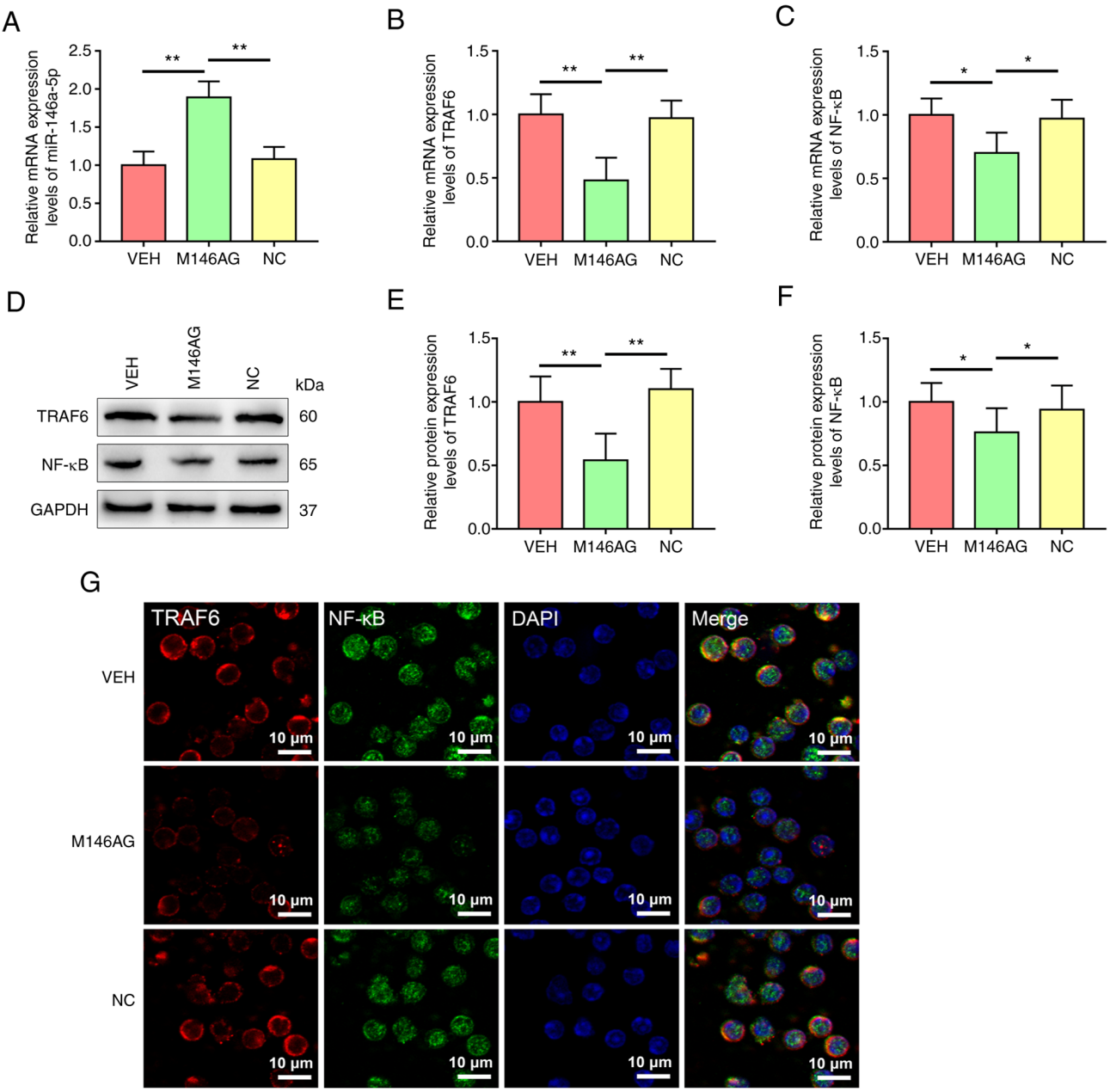

Figure 3. M146AG regulates expression of miR-146a-5p and TRAF6/NF-κB axis components in CD4$^+$ T cells of MRL/lpr mice. (A) Relative miRNA expression level of miR-146a-5p. The relative mRNA expression levels of (B) TRAF6 and (C) NF-κB. (D) Representative western blotting bands of TRAF6/NF-κB axis protein expression levels. Semi-quantified relative protein expression levels of (E) TRAF6 and (F) NF-kB. (G) Protein expression levels of TRAF6 and NF-κB were assessed using immunofluorescence staining (scale bar, 10 μm). All data are presented as the mean ± standard deviation. *P<0.05 and **P<0.01. VEH, vehicle; NC, negative control; miR, microRNA; M146AG, miR-146a-5p agomir; TRAF6, tumor necrosis factor receptor-associated factor 6.

of inflammatory responses, expression levels of IL-17A and Foxp3 in CD4$^+$ T cells of MRL/lpr mice were evaluated. Compared with the VEH and NC group, the level of IL-17A was considerably decreased and protein expression of Foxp3 was significantly increased in CD4$^+$ T cells following M146AG treatment (Fig. 5A-C). Consistent with this, the percentage of Th17 cells significantly decreased and the percentage of Treg cells was significantly increased in the M146AG group compared with the VEH and NC groups (Fig. 5D-G). Furthermore, M146AG treatment significantly lowered the ratio of Th17 to Treg in MRL/lpr mice compared with VEH and NC groups (Fig. 5H). Pearson's correlation analysis demonstrated a significant negative association between Th17/Treg ratio and the mRNA expression levels of miR-146a-5p in the CD4$^+$ T cells of MRL/lpr mice (Fig. 5I). CD4$^+$ T cells of MRL/lpr mice demonstrated a significant positive correlation between Th17/Treg ratio and the relative protein expression of NF-κB (Fig. 5J). These data indicated that M146AG may restore the Th17/Treg balance in MRL/lpr mice by targeting the TRAF6/ NF-κB axis.

Discussion

The inflammatory response caused by T cell subset differentiation and metabolic imbalance is a key cause of SLE. miR-146a-5p in the peripheral blood of patients with SLE

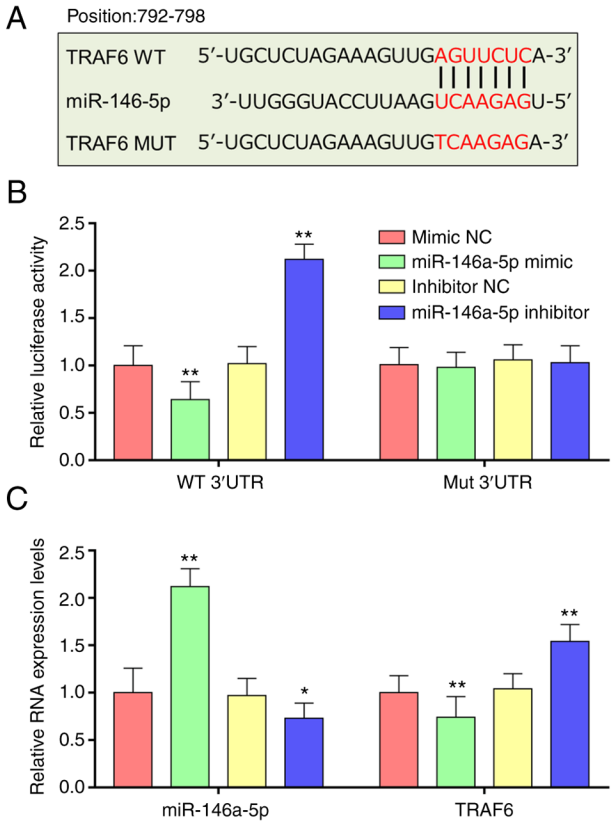

Figure 4. miR-146a-5p directly targets TRAF6. (A) Potential binding sites between miR-146a-5p and TRAF6 3'-UTR were predicted using TargetScan. (B) Dual-luciferase reporter assay demonstrated WT TRAF6-3'-UTR expression following transfection with miR-146a-5p mimic or inhibitor. (C) RNA expression levels of miR-146a-5p and TRAF6 mRNA in 293T cells following miR-146a-5p overexpression and inhibition. All data are presented as the mean ± standard deviation. *P<0.05 and **P<0.01. NC, negative control; miR, microRNA; TRAF6, tumor necrosis factor receptor-associated factor 6; WT, wild-type; MUT, mutant.

is reported to be downregulated, but its direct targets and biological functions are still unclear (22). In the present study, M146AG intervention *in vivo* demonstrated that M146AG treatment repaired the inflammatory response and kidney pathological injury and improved the Treg/Th17 imbalance in peripheral blood of MRL/lpr mice. Furthermore, using bioinformatics tools combined with cell experiments, it was demonstrated that the TRAF6/NF-κB axis was the direct target of miR-146a-5p for immunoregulation in $CD4^{+}$ T cells.

The abnormal metabolism of miRNAs in patients with SLE has received increased attention as the pathogenesis of lupus has been studied in depth (18,34). Therefore, it could be hypothesized that miRNA may be a potential biomarker for the diagnosis of SLE and that a novel SLE therapies with miRNAs as the intervention object could be developed. Thai *et al* (35) reported that elimination of miR-155 in MRL/lpr mice decreases renal inflammation and autoantibody synthesis. Xia *et al* (36) reported that overexpression of miR-326 in MRL/lpr mice results in B cell hyperactivity and serious SLE. Previous studies reported that miR-146a is a significant negative regulator in the immune response and its defect leads to numerous immune disorders (24,37,38). Fu *et al* (24) reported that miR-146a protects the kidney from SLE-induced injury in MRL/lpr mice by regulating both classical and non-classical NF-κB signaling. In the present study, it was demonstrated that M146AG alleviated abnormal renal function and repaired pathological damage of renal tissue in MRL/lpr mice. According to previous reports, the chronic inflammatory response induced by abnormal autoimmune metabolism is the main inducing factor of LN, which primarily manifests as significant upregulation of expression of various pro-inflammatory cytokines, such as IL-6, IL-17A and IFN-γ (39,40). In the present study, it was demonstrated that M146AG intervention markedly downregulated levels of the inflammatory factors IL-6, IFN-γ, TNF-α and IL-17A in both peripheral blood and the renal tissue of MRL/lpr mice. These data indicated that correcting the inflammatory reaction caused by autoimmune disorder is a potential mechanism by which M146AG alleviates LN.

Previous studies have reported that the imbalance of pro-inflammatory and anti-inflammatory T cell subsets, especially Treg and Th17, is a vital reason for the immune homeostasis disorder in autoimmune diseases such as SLE (3,41). Accumulated evidence indicates that the imbalance of Treg and Th17 is involved in the pathogenesis of SLE; however, the root causes of Th17/Treg imbalance in SLE remain unelucidated (3,8). In patients with SLE, the number of Th17 cells and Th17-related inflammatory cytokines such as IL-6 and IL-17 are reported to be increased (27). However, the number of Treg cells and Treg-associated anti-inflammatory cytokines such as TGF-β and IL-10 are reported to be decreased in patients with SLE (42,43). The present study demonstrated that M146AG intervention significantly reversed the imbalance of Th17/Treg in MRL/lpr mice. These data demonstrated that reversing the imbalance of T cell subsets may be a potential mechanism by which M146AG repairs autoimmune disorders in SLE mice.

Previous studies have reported that the inflammatory response mediated by the NF-κB signaling pathway is involved in LN pathogenesis (44,45). Inhibition of the activation of the NOD-like receptor protein 3-mediated inflammasome by inhibiting NF-κB p65 nuclear migration has been reported to alleviate renal inflammation (46). Increasing studies have reported that the NF-κB pathway participates in maintenance of Th17/Treg balance in numerous tissues and organs (47,48). Furthermore, members of the TRAF family are key signaling intermediaries in the NF-κB signaling pathway upstream of the IκB kinase (IKK) complex. NF-κB activation has been reported to be induced by TRAF6 in response to a range of stimuli, such as cell surface or intracellular signals (49). Based on these reports, the TRAF6/NF-κB axis as a target for treatment of SLE and other autoimmune diseases has attracted increased attention (38,50). It has been reported that the levels of miR-146a-5p in renal tissue and peripheral blood are notably decreased in LN patients compared with healthy controls, while the transcriptional activity of TRAF6 and NF-κB is enhanced (37,38). In the present study, upregulation of expression levels of miR-146a-5p by M146AG treatment suppressed activation of the TRAF6/NF-κB axis and corrected the Th17/Treg imbalance in MRL/lpr mice. Similarly, Meng *et al* (51) reported that miR-146a-5p inhibits proliferation of pancreatic ductal adenocarcinoma cells by targeting the 3'-UTR of TRAF6 and downregulation of the TRAF6/NF-κB/p65/P-glycoprotein axis. Liu *et al* (52) also

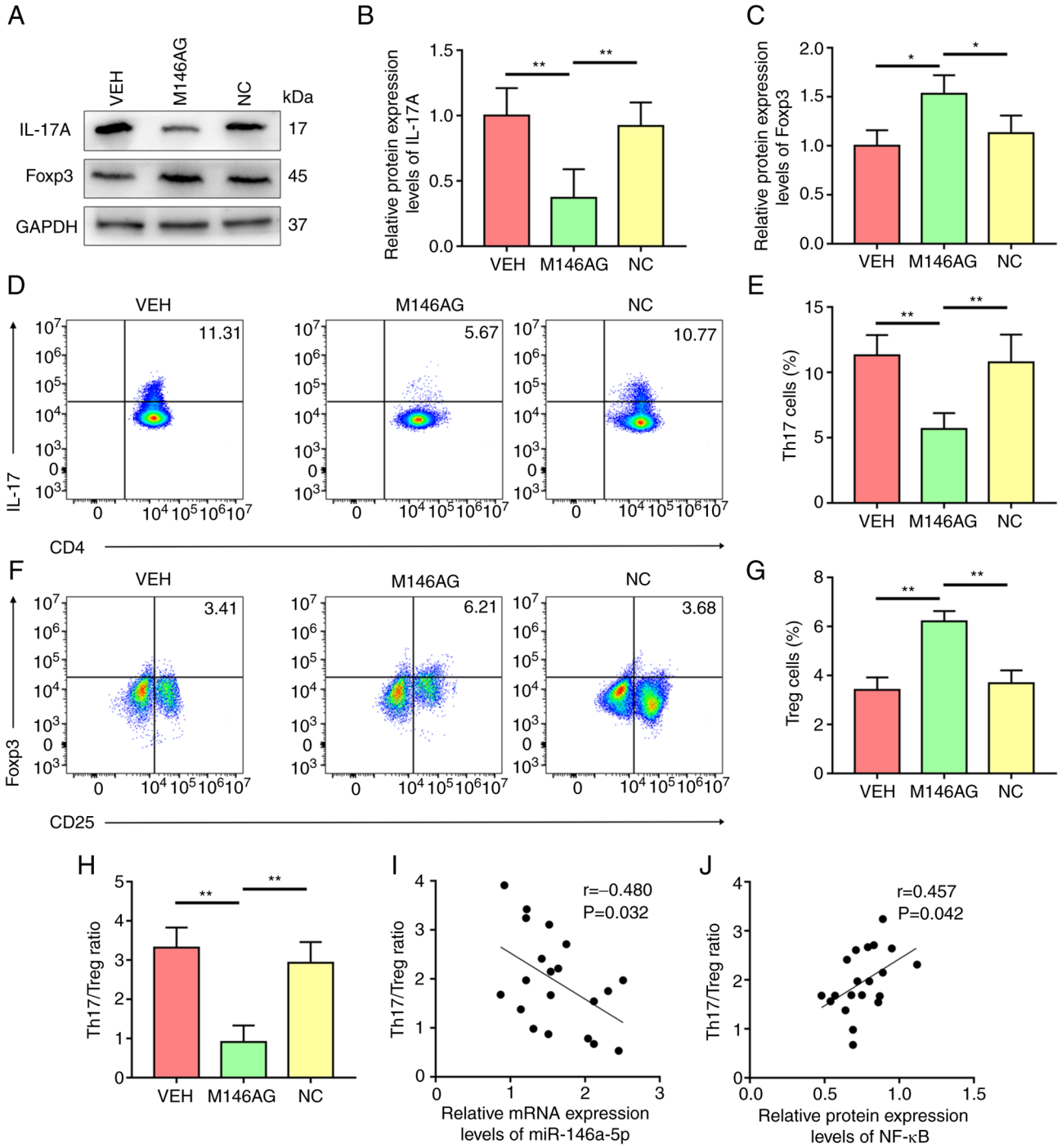

Figure 5. M146AG improves the Treg/Th17 imbalance in MRL/lpr mice. (A) Representative bands of Th17A and Foxp3 protein expression levels assessed using western blotting. The relative protein expression levels of (B) Th17A and (C) Foxp3. (D) Representative flow cytometry dot plots for Th17 cells. (E) Percentage of Th17 cells assessed using flow cytometry. (F) Representative flow cytometry dot plots for Treg cells. (G) Percentage of Treg cells assessed using flow cytometry. (H) Th17/Treg ratio. (I) Pearson correlation analysis between expression of miR-146a-5p and the Th17/Treg ratio. (J) Pearson correlation analysis between the relative protein expression of NF-κB and the Th17/Treg ratio. All data are presented as mean ± standard deviation. *P<0.05 and **P<0.01. VEH, vehicle; NC, negative control; miR, microRNA; M146AG, miR-146a-5p agomir; Treg, T regulatory; Th17, T helper 17.

reported that miR-146a-5p inhibits survival of non-small cell lung cancer cells by directly binding to and suppressing TRAF6. In the present study, the ratio of Th17/Treg in MRL/lpr mice was significantly correlated with expression levels of miR-146a-5p and protein expression levels of NF-κB in $CD4^{+}$ T cells. This was consistent with a previous report that miRNA contributes to the preservation of immunological homeostasis in numerous physiological and pathological situations by the regulation of Th17/Treg balance (3). The aforementioned results suggested that using miRNA as a therapeutic molecule to target TRAF6 or NF-κB to inhibit NF-κB transcriptional activity and inflammatory factor synthesis may be a promising therapeutic strategy for SLE and LN. Nevertheless, the current study was associated with a couple of limitations. For instance, there was a lack of information on the time and dose dependence of M146AG treatment.

In conclusion, the present study demonstrated a potentially novel role for miR-146a-5p in mice with LN, which involved alleviation of the inflammatory response via regulation of the Th17/Treg balance. During this process, the TRAF6/NF-κB axis may be a key target. Therefore, miR-146a-5p may be used as a potential therapeutic target for treatment of LN.

Acknowledgements

Not applicable.

Funding

No funding was received.

Availability of data and materials

The datasets used and/or analyzed during the current study are available from the corresponding author on reasonable request.

Authors' contributions

JT and XL conceived and designed the experiments. JT and FY performed the experiments. FY and XL analyzed the data. XL wrote the paper. All authors have read and approved the final manuscript. JT and XL confirm the authenticity of all the raw data.

Ethics approval and consent to participate

The Ethics Board of Yantai Hospital of Traditional Chinese Medicine approved all experimental procedures (approval no. 2021-09).

Patient consent for publication

Not applicable.

Competing interests

The authors declare that they have no competing interests.

References

1. Mok CC and Lau CS: Pathogenesis of systemic lupus erythematosus. J Clin Pathol 56: 481-490, 2003.
2. Mohan C and Putterman C: Genetics and pathogenesis of systemic lupus erythematosus and lupus nephritis. Nat Rev Nephrol 11: 329-341, 2015.
3. Cheng T, Ding S, Liu S, Li X, Tang X and Sun L: Resolvin D1 improves the Treg/Th17 imbalance in systemic lupus erythematosus through miR-30e-5p. Front Immunol 12: 668760, 2021.
4. Wu S, Ji L, Fan X, Fang S, Bao J, Yuan X, Fan Y and Xie G: Jieduquyuzishen prescription attenuates renal fibrosis in MRL/lpr mice via inhibiting EMT and TGF-β1/Smad2/3 pathway. Evid Based Complement Alternat Med 2022: 4987323, 2022.
5. Li M, Yu D, Ni B and Hao F: Interleukin-1 receptor associated kinase 1 is a potential therapeutic target of anti-inflammatory therapy for systemic lupus erythematosus. Mol Immunol 87: 94-101, 2017.
6. Poissonnier A, Sanséau D, Le Gallo M, Malleter M, Levoin N, Viel R, Morere L, Penna A, Blanco P, Dupuy A, *et al*: CD95-mediated calcium signaling promotes T helper 17 trafficking to inflamed organs in lupus-prone mice. Immunity 45: 209-223, 2016.
7. Wang N and Tian B: Brain-derived neurotrophic factor in autoimmune inflammatory diseases (review). Exp Ther Med 22: 1292, 2021.
8. Shan J, Jin H and Xu Y: T cell metabolism: A new perspective on Th17/Treg cell imbalance in systemic lupus erythematosus. Front Immunol 11: 1027, 2020.
9. Tenbrock K, Rauen T: T cell dysregulation in SLE. Clin Immunol 239: 109031, 2022.
10. Kubo S, Nakayamada S, Yoshikawa M, Miyazaki Y, Sakata K, Nakano K, Hanami K, Iwata S, Miyagawa I, Saito K and Tanaka Y: Peripheral immunophenotyping identifies three subgroups based on T cell heterogeneity in lupus patients. Arthritis Rheumatol 69: 2029-2037, 2017.
11. Xiao JP, Wang DY, Wang XR, Yuan L, Hao L and Wang DG: Increased ratio of Th17 cells to SIGIRR^{+}CD4^{+} T cells in peripheral blood of patients with SLE is associated with disease activity. Biomed Rep 9: 339-344, 2018.
12. Mesquita D Jr, Kirsztajn GM, Franco MF, Reis LA, Perazzio SF, Mesquita FV, Ferreira VDS, Andrade LEC and de Souza AWS: CD4^{+} T helper cells and regulatory T cells in active lupus nephritis: an imbalance towards a predominant Th1 response? Clin Exp Immunol 191: 50-59, 2018.
13. Rafael-Vidal C, Perez N, Altabas I, Garcia S and Pego-Reigosa JM: Blocking IL-17: A promising strategy in the treatment of systemic rheumatic diseases. Int J Mol Sci 21: 7100, 2020.
14. Wang X, Qiao Y, Yang L, Song S, Han Y, Tian Y, Ding M, Jin H, Shao F and Liu A: Leptin levels in patients with systemic lupus erythematosus inversely correlate with regulatory T cell frequency. Lupus 26: 1401-1406, 2017.
15. Liu B, Li J and Cairns MJ: Identifying miRNAs, targets and functions. Brief Bioinform 15: 1-19, 2014.
16. Lu Q, Wu R, Zhao M, Garcia-Gomez A and Ballestar E: miRNAs as therapeutic targets in inflammatory disease. Trends Pharmacol Sci 40: 853-865, 2019.
17. Schell SL and Rahman ZSM: miRNA-Mediated control of B cell responses in immunity and SLE. Front Immunol 12: 683710, 2021.
18. Zhang J, Liu Y and Shi G: The circRNA-miRNA-mRNA regulatory network in systemic lupus erythematosus. Clin Rheumatol 40: 331-339, 2021.
19. Zhou S, Zhang J, Luan P, Ma Z, Dang J, Zhu H, Ma Q, Wang Y and Huo Z: miR-183-5p is a potential molecular marker of systemic lupus erythematosus. J Immunol Res 2021: 5547635, 2021.
20. Cheng T, Ding S, Liu S, Li Y and Sun L: Human umbilical cord-derived mesenchymal stem cell therapy ameliorates lupus through increasing CD4^{+} T cell senescence via MiR-199a-5p/Sirt1/p53 axis. Theranostics 11: 893-905, 2021.
21. Tu Y, Guo R, Li J, Wang S, Leng L, Deng J, Bucala R and Lu L: MiRNA regulation of MIF in SLE and attenuation of murine lupus nephritis with miR-654. Front Immunol 10: 2229, 2019.
22. Tang Y, Luo X, Cui H, Ni X, Yuan M, Guo Y, Huang X, Zhou H, de Vries N, Tak PP, *et al*: MicroRNA-146A contributes to abnormal activation of the type I interferon pathway in human lupus by targeting the key signaling proteins. Arthritis Rheum 60: 1065-1075, 2009.
23. Luo X, Yang W, Ye DQ, Cui H, Zhang Y, Hirankarn N, Qian X, Tang Y, Lau YL, de Vries N, *et al*: A functional variant in microRNA-146a promoter modulates its expression and confers disease risk for systemic lupus erythematosus. PLoS Genet 7: e1002128, 2011.
24. Fu HX, Fan XP, Li M, Liu MJ and Sun QL: MiR-146a relieves kidney injury in mice with systemic lupus erythematosus through regulating NF- κB pathway. Eur Rev Med Pharmacol Sci 23: 7024-7032, 2019.
25. Ye X, Lu Q, Yang A, Rao J, Xie W, He C, Wang W, Li H and Zhang Z: MiR-206 regulates the Th17/Treg ratio during osteoarthritis. Mol Med 27: 64, 2021.
26. Qu X, Han J, Zhang Y, Wang Y, Zhou J, Fan H and Yao R: MiR-384 regulates the Th17/Treg ratio during experimental autoimmune encephalomyelitis pathogenesis. Front Cell Neurosci 11: 88, 2017.
27. Wang D, Huang S, Yuan X, Liang J, Xu R, Yao G, Feng X and Sun L: The regulation of the Treg/Th17 balance by mesenchymal stem cells in human systemic lupus erythematosus. Cell Mol Immunol 14: 423-431, 2017.
28. Geng L, Tang X, Zhou K, Wang D, Wang S, Yao G, Chen W, Gao X, Chen W, Shi S, *et al*: MicroRNA-663 induces immune dysregulation by inhibiting TGF-β1 production in bone marrow-derived mesenchymal stem cells in patients with systemic lupus erythematosus. Cell Mol Immunol 16: 260-274, 2019.

29. Remuzzi G, Zoja C, Gagliardini E, Corna D, Abbate M and Benigni A: Combining an antiproteinuric approach with mycophenolate mofetil fully suppresses progressive nephropathy of experimental animals. J Am Soc Nephrol 10: 1542-1549, 1999.
30. Xiong Y, Xiong Y, Zhang H, Zhao Y, Han K, Zhang J, Zhao D, Yu Z, Geng Z, Wang L, *et al*: hPMSCs-derived exosomal miRNA-21 protects against aging-related oxidative damage of $CD4^+$ T cells by targeting the PTEN/PI3K-Nrf2 axis. Front Immunol 12: 780897, 2021.
31. Wang Y, Xiong Y, Zhang A, Zhao N, Zhang J, Zhao D, Yu Z, Xu N, Yin Y, Luan X and Xiong Y: Oligosaccharide attenuates aging-related liver dysfunction by activating Nrf2 antioxidant signaling. Food Sci Nutr 8: 3872-3881, 2020.
32. Wang Y, Zhao N, Xiong Y, Zhang J, Zhao D, Yin Y, Song L, Yin Y, Wang J, Luan X and Xiong Y: Downregulated recycling process but not de novo synthesis of glutathione limits antioxidant capacity of erythrocytes in hypoxia. Oxid Med Cell Longev 2020: 7834252, 2020.
33. Livak KJ and Schmittgen TD: Analysis of relative gene expression data using real-time quantitative PCR and the 2(-Delta Delta C(T)) method. Methods 25: 402-408, 2001.
34. Sui W, Liu F, Chen J, Ou M and Dai Y: Microarray technology for analysis of microRNA expression in renal biopsies of lupus nephritis patients. Methods Mol Biol 1134: 211-220, 2014.
35. Thai TH, Patterson HC, Pham DH, Kis-Toth K, Kaminski DA and Tsokos GC: Deletion of microRNA-155 reduces autoantibody responses and alleviates lupus-like disease in the Fas(lpr) mouse. Proc Natl Acad Sci USA 110: 20194-20199, 2013.
36. Xia Y, Tao JH, Fang X, Xiang N, Dai XJ, Jin L, Li XM, Wang YP and Li XP: MicroRNA-326 upregulates B cell activity and autoantibody production in lupus disease of MRL/lpr mice. Mol Ther Nucleic Acids 11: 284-291, 2018.
37. Zhu Y, Xue Z and Di L: Regulation of MiR-146a and TRAF6 in the diagnose of lupus nephritis. Med Sci Monit 23: 2550-2557, 2017.
38. Zheng CZ, Shu YB, Luo YL and Luo J: The role of miR-146a in modulating TRAF6-induced inflammation during lupus nephritis. Eur Rev Med Pharmacol Sci 21: 1041-1048, 2017.
39. Cai Z, Wong CK, Dong J, Jiao D, Chu M, Leung PC, Lau CBS, Lau CP, Tam LS and Lam CWK: Anti-inflammatory activities of Ganoderma lucidum (Lingzhi) and San-Miao-San supplements in MRL/lpr mice for the treatment of systemic lupus erythematosus. Chin Med 11: 23, 2016.
40. Zickert A, Amoudruz P, Sundstrom Y, Ronnelid J, Malmstrom V and Gunnarsson I: IL-17 and IL-23 in lupus nephritis-association to histopathology and response to treatment. BMC Immunol 16: 7, 2015.
41. Talaat RM, Mohamed SF, Bassyouni IH and Raouf AA: Th1/Th2/Th17/Treg cytokine imbalance in systemic lupus erythematosus (SLE) patients: Correlation with disease activity. Cytokine 72: 146-53, 2015.
42. Ohl K and Tenbrock K: Regulatory T cells in systemic lupus erythematosus. Eur J Immunol 45: 344-355, 2015.
43. Choi Y, Jung JH, Lee EG, Kim KM and Yoo WH: 4-phenylbutyric acid mediates therapeutic effect in systemic lupus erythematosus: Observations in an experimental murine lupus model. Exp Ther Med 21: 460, 2021.
44. Sun F, Teng J, Yu P, Li W, Chang J and Xu H: Involvement of TWEAK and the NF-κB signaling pathway in lupus nephritis. Exp Ther Med 15: 2611-2619, 2018.
45. Sun L, Zou LX, Han YC, Wu L, Chen T, Zhu DD and Hu P: A20 overexpression exerts protective effects on podocyte injury in lupus nephritis by downregulating UCH-L1. J Cell Physiol: Feb 25, 2019 (Epub ahead of print).
46. Zhang H, Liu L and Li L: Lentivirus-mediated knockdown of FcgammaRI (CD64) attenuated lupus nephritis via inhibition of NF-κB regulating NLRP3 inflammasome activation in MRL/lpr mice. J Pharmacol Sci 137: 342-349, 2018.
47. Cui C, Zhang D, Sun K, Li H, Xu L, Lin G, Guo Y, Hu J, Chen J, Nong L, *et al*: Propofol maintains Th17/Treg cell balance and reduces inflammation in rats with traumatic brain injury via the miR1453p/NFATc2/NF-κB axis. Int J Mol Med 48: 135, 2021.
48. Chen C, Hu N, Wang J, Xu L, Jia XL, Fan X, Shi JX, Chen F, Tu Y, Wang YW and Li XH: Umbilical cord mesenchymal stem cells promote neurological repair after traumatic brain injury through regulating Treg/Th17 balance. Brain Res 1775: 147711, 2022.
49. Napetschnig J and Wu H: Molecular basis of NF-κB signaling. Annu Rev Biophys 42: 443-468, 2013.
50. Dong C, Zhou Q, Fu T, Zhao R, Yang J, Kong X, Zhang Z, Sun C, Bao Y, Ge X, *et al*: Circulating exosomes derived-miR-146a from systemic lupus erythematosus patients regulates senescence of mesenchymal stem cells. Biomed Res Int 2019: 6071308, 2019.
51. Meng Q, Liang C, Hua J, Zhang B, Liu J, Zhang Y, Wei M, Yu X, Xu J and Shi S: A miR-146a-5p/TRAF6/NF-kB p65 axis regulates pancreatic cancer chemoresistance: Functional validation and clinical significance. Theranostics 10: 3967-3979, 2020.
52. Liu X, Liu B, Li R, Wang F, Wang N, Zhang M, Bai Y, Wu J, Liu L, Han D, *et al*: miR-146a-5p plays an oncogenic role in NSCLC via suppression of TRAF6. Front Cell Dev Biol 8: 847, 2020.